J Mater Sci (2007) 42:1884–1889
DOI 10.1007/s10853-006-1321-z

NONSTOICHIOMETRIC COMPOUNDS

Accommodation of non-stoichiometry in TiN_{1-x} and ZrN_{1-x}

Nicholas J. Ashley · Robin W. Grimes · Ken J. McClellan

Received: 25 November 2005 / Accepted: 6 March 2006 / Published online: 18 January 2007

Abstract Atomic scale computer simulations, based on density functional calculations, are used to investigate the variation of lattice parameter and bulk modulus with nitrogen deficient non-stoichiometry in titanium and zirconium nitrides. Results assuming a simple distribution of nitrogen vacancies best reflect the remarkably small observed changes in lattice parameter over the whole stoichiometry range for both materials. These are facilitated by small charge transfer to the cations immediately surrounding the nitrogen vacancy and small accompanying lattice relaxations. Conversely variations in bulk modulus are considerable but can be correlated, via a simple function, to the change in materials density.

Introduction

Titanium and zirconium nitrides should be simple materials, after all, they both have the rock salt structure [1–11]. It is known experimentally, however, that they exhibit a remarkably broad range of non-stoichiometry. If they are described using the formula MN_{1-x} where M = Ti or Zr, then x assumes values from 0 to as much as 0.35 [4–11]. Within this range these materials maintain their long-range rock salt structure symmetry.

In comparison, $Fe_{1-x}O$, which also has the rock salt structure and is considered to have exceptional non-stoichiometry, is stable within the more restricted range $0.05 < x < 0.15$ [12]. Furthermore, $Co_{1-x}O$, again rock salt, has been the subject of numerous studies due to its non-stoichiometry, but provides only the range $0.001 < x < 0.05$ [13].

The aim of this work is to investigate atomic scale models for nitrogen deficient non-stoichiometry in zirconium and titanium nitrides and test these against the available experimental data. A successful model may then lead to an understanding of the factors that make such a broad range of non-stoichiometry possible.

Experimental data

As described in a recent review [10] titanium nitride exhibits extensive nitrogen-deficient non-stoichiometry TiN_{1-x} [3–9]. It has been suggested that this large degree of non-stoichiometry is facilitated by simple anion vacancies [7]. This conclusion, however, was drawn from simple density calculations based on experimental information such as lattice parameter and symmetry. It also seems that it is possible to generate compositions in which the titanium ratio is greater than unity [10]. However, a mechanism responsible for this has not been suggested.

Extensive nitrogen-deficient non-stoichiometry has also been identified in zirconium nitride and again attributed to vacancies on the nitrogen lattice sites [7]. The formation of zirconium-deficient materials have

N. J. Ashley · R. W. Grimes (✉)
Department of Materials, Imperial College, London SW7 2BP, UK
e-mail: r.grimes@ic.ac.uk

K. J. McClellan
Los Alamos National Laboratory, MST-8 Mail Stop G755, Los Alamos, NM 87544, USA

also been suggested [14]. More recent work [2, 11] however, was unable to confirm such single phase stoichiometry but rather resulted in the formation of either an insulating transparent single phase with composition Zr_3N_4 or a mixed phase ZrN, Zr_3N_4 material. Therefore, as a first step towards establishing our approach for investigating these systems we have chosen to model only the nitrogen deficient non-stoichiometry.

Methodology

Simulation technique

This study requires a technique that can reproduce the complex bonding characteristics of a metal nitride material. It is for this reason that we have used a quantum mechanical approach. As a consequence, the number of atoms that can be modelled explicitly is restricted.

In this study, we have used super-cells containing up to 32 ions, which are repeated through space using periodic conditions. Calculations were performed within the density functional approach (DFT) [15] using the generalized gradient approximation corrected exchange correlation functional of Perdew and Wang [16]. A Monkhurst-Pack grid was used to define the density of the k-points, which in this case was approximately 0.04 $Å^{-1}$. The plane wave basis set, which was expanded to a cut-off of 450 eV, was used in combination with ultra-soft pseudo potentials. The simulations were performed under constant pressure conditions so that unit cell parameters along with cation and anion fractional coordinates were allowed to relax via energy minimization. Consequently the calculations were performed in the static limit, which is the most significant approximation in this study. Simulations were carried out using the DFT package CASTEP [17].

Defect structures

In the initial calculations a single defect was introduced into a 1 × 1 × 1 (single fcc full unit cell of the rock salt structure), a 2 × 1 × 1 (two unit cells adjacent along the *x*-axis) and a 2 × 2 × 1 unit cell. These structures therefore contain a uniform distribution of defects as a consequence of the periodic conditions.

Higher concentrations of defects within these cells were modelled by including multiple defects. This also results in our being able to construct alternate configurations of the defect distribution at a given overall defect concentration. For example, although the 2 × 1 × 1 cell with two defects has the same defect concentration as a 1 × 1 × 1 cell with one defect, it is possible to arrange the two defects in the 2 × 1 × 1 cell in four distinct ways (see Fig. 1). These calculations yield a range of predicted lattice parameters for a given stoichiometry. The energy associated with each structure was also calculated; relative energies and relative degeneracies contribute towards the likelihood of a given configuration occurring. With this information a thermodynamic average can be computed using Eq. 1, which yields a configurationally averaged lattice parameter

$$a = \frac{\sum n_i [e^{\frac{-\Delta E_i}{kT}} (a_i \cdot b_i \cdot c_i)^{\frac{1}{3}}]}{\sum n_i e^{\frac{-\Delta E_i}{kT}}} \quad (1)$$

where ΔE_i is the lattice energy of configuration i relative to the configuration with the lowest energy, n_i is its relative degeneracy, k is Boltzmann's constant, T is temperature and a_i, b_i and c_i represent the energy minimised unit cell lengths for configuration i [18, 19]. In this way we are able to approximately account for the distribution of defects, the disorder, that will be

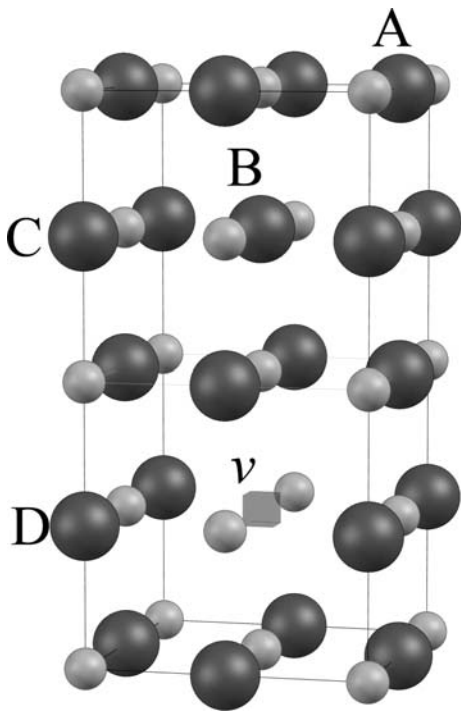

Fig. 1 Configurations of vacancy clusters in an M_8N_8 periodic cell (large atoms are nitrogen, small atoms metal). If a nitrogen vacancy is positioned at *v*, the cell provides four unique positions for a second vacancy: A, B, C or D. The overall compositions of this cell would then be $MN_{0.75}$ (M = Ti or Zr)

apparent in a real material by averaging over a number of specific ordered distributions. The temperature assumed for the averaging was 1000 K. At temperatures below 1000 K, in these types of ceramics, atoms are no longer able to migrate through the lattice. Furthermore, predicted lattice parameters generated via Eq. 1, within 200 K of this temperature, show little variation. Consequently 1000 K is an acceptable representative temperature at which the distribution becomes effectively frozen.

An effective stoichiometry MN_{1-x}, where $0 < x < 0.5$, can be facilitated by three types of defects: nitrogen vacancies (V_N), anti-site defects (titanium ions occupying nitrogen sites, Ti_N) or titanium interstitial ions (Ti_i). In terms of the defect properties of a compact lattice, nitrogen vacancies (Eq. 2) would be typical of what is expected from an ionic or partially ionic (semi-covalent) ceramic. Interstitial titanium (Eq. 3) is typical of a metallic system (or a ceramic with an open structure—of which the rock salt structure is certainly not an example). Anti-site defects (Eq. 4) often form in semiconducting systems. In the associated equations the subscript indicates the usual lattice site of a specified ion and N_2 indicates one molecule of nitrogen will be generated by the reaction.

$$N_N \rightarrow V_N + \frac{1}{2}N_2 \quad (2)$$

$$MN \rightarrow M_i + \frac{1}{2}N_2 \quad (3)$$

$$MN + N_N \rightarrow M_N + N_2 \quad (4)$$

Results

The mechanism of non-stoichiometry

Figure 2 shows the predicted lattice parameter of TiN_{1-x} as a function of composition (x) for the three defect mechanisms identified above (configurationally averaged for the vacancy mechanism only). These are compared with the experimental data identified in the section concerning experimental data. It is at once apparent that only the vacancy mechanism reproduces the observed lattice parameter data for nitrogen deficient non-stoichiometric compositions.

A similar trend is predicted in Fig. 3, which shows the lattice parameter results for ZrN_{1-x} as a function of composition (x). Again there is a clear correlation between the experimental results discussed previously and the lattice parameters predicted using a vacancy mechanism. Thus, as far as defect accommodation is concerned, both TiN_{1-x} and ZrN_{1-x} are behaving as classic compact ionic or semi-ionic ceramics.

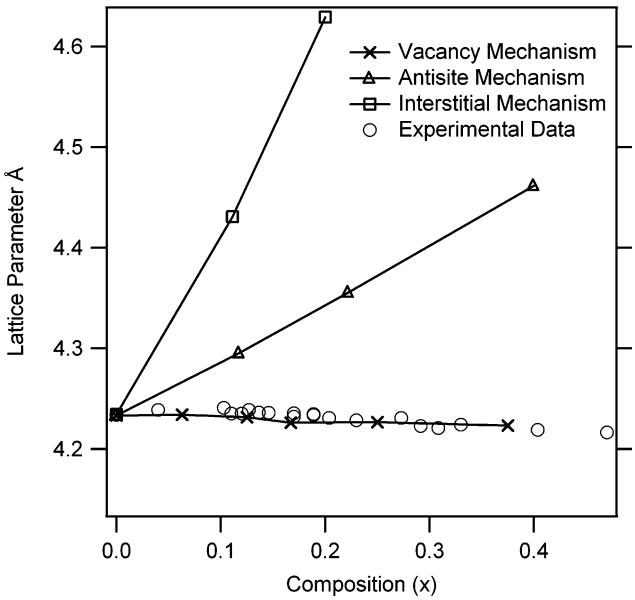

Fig. 2 Lattice parameter predictions for non-stoichiometry in TiN_{1-x} assuming three different mechanisms. Experimental data from [3, 9]

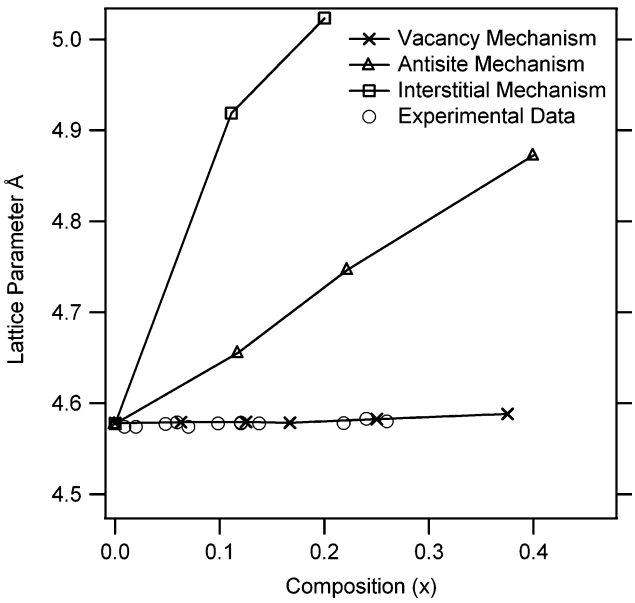

Fig. 3 Lattice parameter predictions for non-stoichiometry in ZrN_{1-x} assuming three different mechanisms. Experimental data from [7]

If the change in lattice parameter is approximated to be linear with change in stoichiometry (x), then the lattice parameters of TiN_{1-x} and ZrN_{1-x} can be described by the following equation:

$$a_{MN_{1-x}} = a_{MN} - yx \quad (5)$$

where $a_{MN_{1-x}}$ is the lattice parameter at composition x, a_{MN} is the lattice parameter at the stoichiometric composition, and y is a constant. The value of the constant y for TiN_{1-x} is –0.0287 and for ZrN_{1-x} 0.0254. The small magnitude of the y values reflects the remarkably small change in lattice parameters over the broad stoichiometric range.

The nitrogen vacancy mechanism

Figure 4 shows the agreement between the vacancy mechanism predicted lattice parameter and experimental data for TiN_{1-x} in more detail (including the concentrations where it was possible to model alternate configurations). It is apparent that the agreement between theory and experiment is exceptional especially considering the way in which we have imposed a limited number of specific orders on the nitrogen vacancy distribution. In a completely disordered material the vacancies would be randomly distributed with many different local alternate configurations and clusters being formed. The small spread of lattice parameter values associated with these limited number of different specific defect configurations is therefore noteworthy, and it is tempting to speculate that in these two systems, different imposed order schemes lead to very similar lattice parameters. Unfortunately given the present restriction in cell size it is not possible to investigate this further.

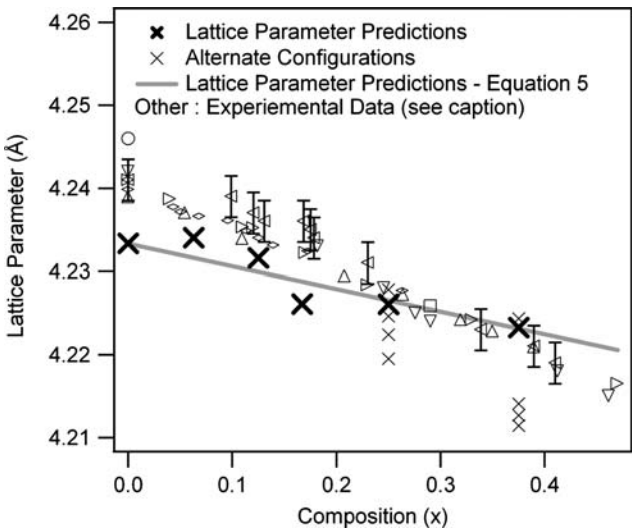

Fig. 4 Lattice parameter predictions for non-stoichiometry in TiN_{1-x} assuming the vacancy mechanism. Experimental data from: ○ Duwez and Odell [3], □ Holmberg [4], △ Nagakura et al. [5], ▽ Arbuzov et al. [6], ◁ Christensen et al. [7], ▷ Lengauer [8] and ◇ Jiang et al. [9]

It is now necessary to consider the local lattice response to the inclusion of a nitrogen vacancy. It was found that, after allowing for complete lattice relaxation, the 1st neighbour ions (metal) were displaced by only 0.02 Å radially outwards away from the vacant nitrogen site. This is a small movement compared to lattice relaxation exhibited around anion vacancies in equivalent ionic systems. For example, in MgO, which also has the rock salt structure, the cations adjacent to an oxygen vacancy would be expected to move by as much as 0.2 Å [20].

In addition to the atomic relaxation, it is also interesting to consider how the nitrogen vacancy charge compensation is distributed. Mulliken population analysis suggests that in the perfect lattice nitrogen has a net charge of approximately –1. This is, of course, far from the formal nitrogen valency of –3. The formation of a nitrogen vacancy creates a total defect charge within the lattice of –1. This is accommodated through a change in the charge of all the metal ions that immediately neighbour the nitrogen vacancy (no change in second neighbour nitrogen charge was predicted). Given the moderate ionicity and six neighbour cations, this leads to a small local change in the overall charge density of the lattice, and presumably to the small ion displacements and hence small changes in the overall lattice parameter (less than 1% over the whole range of stoichiometry). (Note: Mulliken populations calculated for plane wave simulations are approximate. That is why we emphasise only broad changes in charge distributions, which are certainly more reliable, and do not report actual population values.)

Figure 5 shows the agreement between the vacancy mechanism predicted lattice parameter and experimental data for ZrN_{1-x}. This behaviour is very similar to that of the TiN_{1-x} compositions, although, in the case of ZrN_{1-x} there is a trend for the lattice parameter to increase slightly with the reduction of nitrogen content, although the change is less than 0.3% over the whole stoichiometry range. This is the opposite to the observed trend downward for TiN_{1-x} although the magnitude still emphasises how small the lattice volume changes are considering the enormous changes in stoichiometry. Interestingly this behaviour is not what would be expected from an ionic system where vacancy defects are usually accompanied by considerable lattice expansion or from a metal where atoms

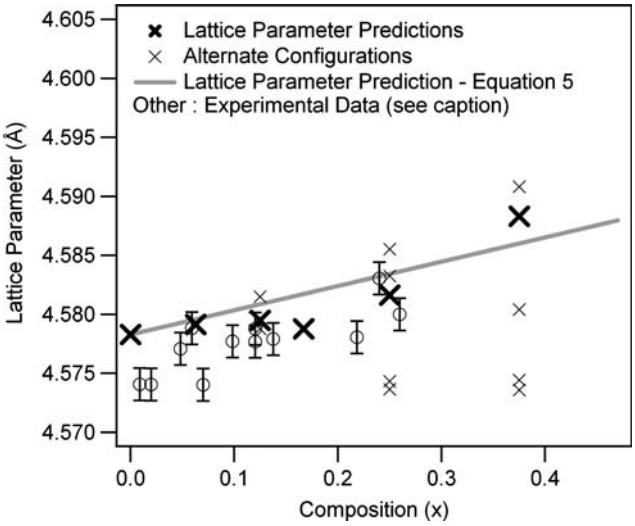

Fig. 5 Lattice parameter predictions for non-stoichiometry in ZrN_{1-x} assuming the vacancy mechanism. Experimental data from: ○ Christensen et al. [7]

relax inwards. Presumably this balance reflects the partial ionicity, partial delocalised nature of the bonding electrons in these systems.

We now return to the issue of alternative configurations. Figure 1 shows the atomic arrangements of the four configurations at a stoichiometry of $MN_{0.75}$. As previously stated and shown in Figs. 4 and 5, the predicted lattice parameters are all similar. By comparing the energies, however, we find that for both TiN and ZrN the most stable configuration is that in which the second vacancy is at site C. For TiN and ZrN, respectively, configuration C is 0.04 and 0.07 eV more stable (i.e. lower in energy) than A. Configurations B and D are between 0.1 and 0.4 eV less stable. Thus, although the different configurations all yield similar lattice parameters, they are by no means all equally likely to be present (hence our use of Eq. 1). What differentiates geometry C from others is that the vacancies share no first neighbour metal atoms. All other configurations considered have between two and four common metal first neighbour atoms. As stated previously the first neighbour metal atoms assume the excess charge due to the vacancy. Therefore, if two vacancies have a common metal first neighbour atom this species will have two sources from which charge is being donated.

The existence of such short-range configurational preference may conceivably give rise to a degree of short-range order (as reported in ZrN by Li and Howe [21]). The fact, however, that two different configurations are so close in energy and lattice parameter, indicates it is unlikely that long-range order would be established. To achieve long-range order there must be either a clear energetic preference for a specific configuration (not the case here) or those configurations with similar energies must give rise to different lattice parameters i.e. they give rise to different long-range strain fields, which will thereby establish a specific preference driving forces (therefore also not the case here).

Changes in bulk modulus

Although the lattice parameter changes are small, the change in density as a function of non-stoichiometry is certainly pronounced (assuming the vacancy mechanism). Associated with this reduction in density is a pronounced reduction in the bulk modulus of the material (predicted values are presented in Fig. 6 using the lattice parameter variation derived by Eq. 5). A relationship between the bulk modulus and density of these materials can be derived as follows:

$$B_{\mathrm{MN}_{1-x}} = B_{\mathrm{MN}} - \alpha(\Delta\rho) + \beta(\Delta\rho)^2 \quad (6)$$

where $B_{\mathrm{MN1}\text{-}x}$ is the bulk modulus of a material with composition x, B_{MN} the bulk modulus for stoichiometric MN, $\Delta\rho = \rho_{\mathrm{MN}} - \rho_{\mathrm{MN1}\text{-}x}$, and α and β are constants specific to each material. For TiN_{1-x} the value of the constants α and β are –0.2404 and 0.0004, respectively, while for ZrN_{1-x} they are 0.1805 and 0.0001. In both cases, the considerably larger values

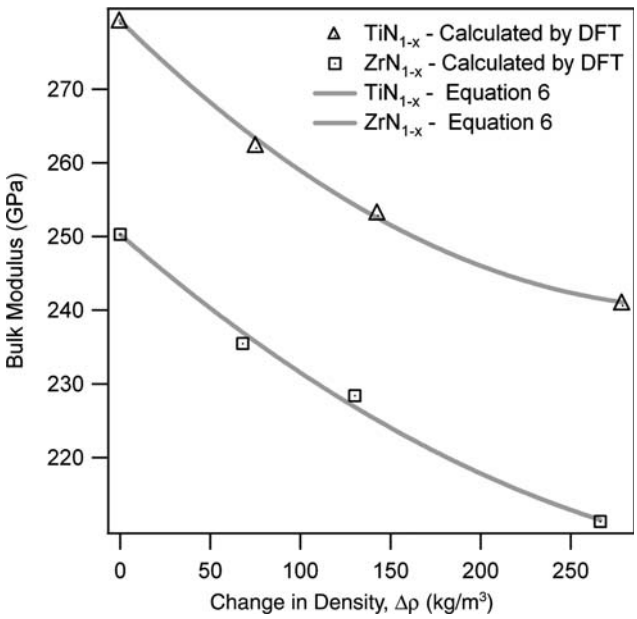

Fig. 6 Variations in bulk modulus predicted as a function of density in TiN_{1-x} and ZrN_{1-x}

of α than β demonstrates that the linear term is by far the dominant factor in reducing bulk modulus. Presumably this is a consequence of the local manner in which these materials accommodate the non-stoichiometry.

The bulk modulus relationships, shown in Fig. 6 provide a simple way to predict this mechanical property by measuring density. It is, however, also important to bear in mind that computational techniques are often better at predicting trends rather than absolute values. As such, these relationships could be used in combination with experimental values of bulk modulus for the stoichiometric materials, B_{MN}. Also, similar relationships for other mechanical properties (e.g. Young's modulus) could be derived in the future now that the atomic scale mechanism responsible for the non-stoichiometry has been established.

Conclusions

It is clear that, despite the enormous range of non-stoichiometry, a simple mechanism consisting of a distribution of nitrogen vacancies can described the variation of lattice parameter as a function of x in MN_{1-x} for both titanium and zirconium nitrides. Other possible mechanisms based on interstitial defects or anti-site defects have been discounted. Changes in nitrogen deficient stoichiometry are facilitated by small changes in the electronic charge of the neighbouring metal ions within the structure. These ions are not, however, displaced to any great extent from their lattice sites. Vacancies within these structures therefore reduce the density of the lattice, and this is reflected in a reduction of the bulk modulus of the materials.

Acknowledgements NJA is grateful to the EPSRC Faraday Mini-Waste Partnership for providing a studentship and The Worshipful Company of Armourers and Brasiers for their support. This work was partially funded by the Advanced Fuel Cycle Initiative. Ray Withers, Kurt Atkinson and Chris Stanek are thanked for informative discussions. Computing resources were provided by the MOTT2 facility (EPSRC Grant GR/S84415/01).

References

1. Christensen AN (1975) Acta Chem Scand A 29:563
2. Johansson BO, Hentzell HTG, Harper JME, Cuomo J (1986) J Mater Res 1(3):442
3. Duwez P, Odell F (1950) J Electrochem Soc 97(10):299
4. Holmberg B (1962) Acta Chem Scand 16:1255
5. Nagakura S, Kusunoki T, Kakimoto F, Hirotsu Y (1975) J Appl Crystallogr 8:65
6. Arbuzov MP, Golub SY, Khaenko BV (1977) Inorg Mater 13(10):1434
7. Christensen AN, Fregerslev S (1977) Acta Chem Scand A 31:861
8. Lengauer W(1992) J Alloys Compd 186(2):293
9. Jiang C-C, Goto T, Hirai T (1993) J Alloys Compd 190(2):197
10. Wriedt H, Murray JL (1987) Bull Alloy Phase Diag 8(4):378
11. Benia HM, Guemmaz A, Schmerber G, Mosser A, Parlebas JC (2004) Catal Today 89(3):307
12. Darken LS, Gurry RW (1945) J Am Ceram Soc 67:1398
13. Choi JS, Yo CH (1974) Inorg Chem 13(7):1720
14. Straumanis JS, Faunce CA, James WJ (1966) Inorg Chem 5(11):2027
15. Hohenburg R, Kohn W (1964) Phys Rev 136:B864
16. Perdew JP (1991) Physica B 172(1–2):1
17. Payne MC, Teter MP, Allan DC, Arias TA, Joannopoulos JD (1992) Rev Mod Phys 64:1045
18. Zacate MO, Grimes RW (2000) Philos Mag A 80(4):797
19. Mohn CE, Allan NL, Freeman CL, Ravindran P, Stlen S (2005) J Solid State Chem 178(1):346
20. Grimes RW, Catlow CRA, Stoneham AM (1989) J Phys Condens Matter 1(40):7367
21. Li P, Howe JM (2002) Acta Mater 50(17):4231